Original Research Article

Understanding urban expansion and its landscape responses with long-term Landsat data in Guangzhou, China

Abstract: Quantifying the spatio-temporal pattern of urban expansion is essential to understanding the ecological consequences of urbanization and supporting optimal urban management strategies. As one of the most developed regions in China, Guangzhou has experienced rapid urban expansion over the past decades. However, little is known about the detailed process of urban expansion across long-term periods. Combining remote sensing data with GIS techniques, we attempted to quantify the spatio-temporal pattern of urban expansion in Guangzhou. We mapped the urban landscape in Guangzhou using Landsat images between 1973 and 2017. The urban land developed and change process was also examined, including urban expansion direction, urban expansion types, and landscape responses to urban expansion. The results showed that the building nearly increased by 90-fold from 1973 to 2017, and over half of the newly developed buildings mainly came from farmland. Edge expansion is the main type of urban growth. The urban trajectory shows that the expansion mainly occurred in the southwest to northeast direction. Urban growth led to radical changes in the urban landscape, leading to sharp decreases in soil and farmland. The results from this study provide key information for future planning to make eco-friendly megacities as well as sustainable development.
Keywords: Urban expansion; Landscape response; Guangzhou; Landsat

1 Introduction

In recent decades, unprecedented urban expansion has led to the modification of the Earth's surface structure [1, 2]. Urban land accounts for merely a small part of the Earth's land surface, but the acceleration of the urbanization process has had a significant impact on terrestrial ecosystems at different scales [3-5], resulting in reduced biological diversity, impacted ecosystem services and function, changed biogeochemical cycles and climate [6-10]. With fast economic and population growth in China, rapid urban land expansion has tremendously changed the regional and continental environmental systems, leading to a lot of negative environmental impacts such as loss of arable land, fragmented habitats, and elevated land surface temperature [11]. The rapid urban land expansion has threatened sustainable development [12, 13]. Therefore, given such political and sustainable development demands, accurate and updated urban expansion information and landscape change response information are crucially important to support sustainable development and preserve ecological and environmental conditions for researchers and governors [12].

As the core of Pearl River Delta urban agglomeration and a pilot area of Guangdong-Hong Kong-Macao Greater Bay, Guangzhou is an excellent example for studying urban expansion related to its process, because it is one of the largest metropolitans and rapidly developing areas in China or even the world. The socioeconomic factor was the primary driving force that directly and indirectly affected Guangzhou's composition of land cover. Following the urban sprawl, a large number of buildings have become one of the most dominant urban landscapes in Guangzhou. Continuous urban expansion has led to many environmental issues in Guangzhou over the few decades, including large arable land loss, urban heat islands, and water pollution [14-16]. As the size and number of the buildings continue to grow, these impacts on the natural systems will become more apparent. Urban expansion brings huge pressure to the environment and ecological systems. The rapid pace of

building growth is reshaping the morphology and function of the urban area. Guangzhou faces a huge challenge in maintaining trade-offs between regional development and ecological benefits, highlighting the need for a clear understanding on the urban expansion process. Therefore, in-depth studies of urban expansion patterns are essential to promote sustainable urban development in Guangzhou.

Given the rapid urban development in Guangzhou, accurate and long-term data on the dynamics of urban expansion is highly vital to optimize land use patterns and to promote effective development to ensure urban sustainability. Moreover, a comprehensive characterizing urban expansion process will provide basic and valuable information on monitoring of urban planning effects and modeling urban growth in Guangzhou. We first mapped the urban landscape with an integrated method, and the changes in urban landscape was also evaluated. Then, we examined the spatio-temporal patterns of urban expansion, mainly including expansion types, and expansion direction (or trajectory).

2 Materials and methods

2.1 Study area and data source

Guangzhou is located between 112°57′1.1″-114°3′19.57″E and 22°33′35.32″-23°56′1.99″N, and covers an area of about 7,434.4 km^2 (Fig.1). Guangzhou, as the center of Pearl River Delta and the capital of Guangdong province, is the cultural, economic, and political center of south China. Guangzhou comprises of 12 districts, namely: Yuexiu, Tianhe, Haizhu, Liwan, Huangpu, Luogang, Panyu, Nansha, Baiyun, Huadu, Zengcheng and Conghua. Guangzhou has a typical sub-tropical maritime monsoon climate, in which persistent rain and clouds in spring and summer (two wet seasons) are a prominent climate feature [17]. The topography in Guangzhou has a low elevation in the south, but high in the northeast.

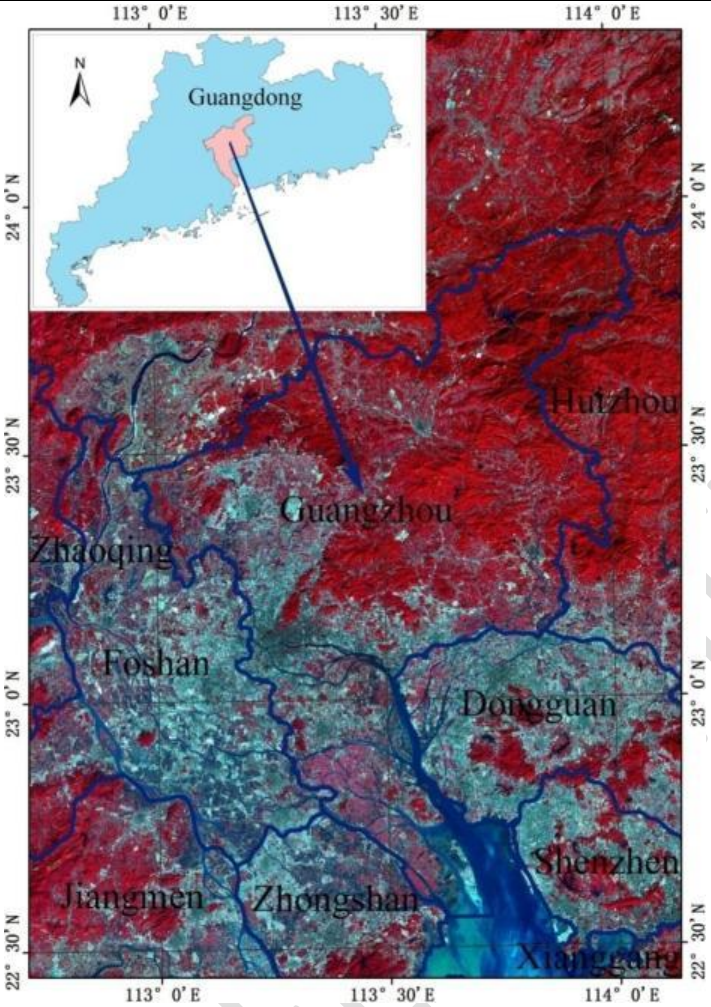

Fig.1 Location of the study area (The false-color image is the Landsat-5TM image collected on November 02, 2009).

Understanding the complex processes of urban expansion requires long-term records [18]. Eighteen Landsat images from nine periods from the U.S. Geological Survey (USGS) website were used as imagery sources to monitor urban expansion over a 44-year period (Table 1). All of the used images were selected because they were cloud-free or cloud-few from October to December in each study period. Other ancillary data include the Guangzhou administrative map (2005) for delineation of the study boundary and the high-resolution image (2009) from Google Earth for selecting classification samples and assessing classification accuracy.

Table 1 List of Landsat images used in this study.

Years	Sensor	Acquired date (yyyy/mm/dd)	Number of GCP's for registration	Geometric registration RMS error
1973	MSS	1973/10/25	16	±0.45
1979	MSS	1979/10/19	15	±0.49
1988	TM	1988/12/10	10	±0.33
1994	TM	1994/10/24	15	±0.35
2000	TM	2000/10/08	7	±0.17
2005	TM	2005/11/23	7	±0.005
2009	TM	2009/11/02	~	Master image
2013	OLI	2013/11/29	6	±0.002

2017	OLI	2017/10/23	9	±0.061

2.2 Images pre-processing

The surface reflectance (SR) data of 2009 were obtained from the USGS EROS Science Products Architecture (ESPA, https://espa.cr.usgs.gov/), and the rest were obtained from the USGS Earth Explorer (https://earthexplorer.usgs.gov/). Except for the 2009 SR data, the original digital numbers of these images were converted to the atmospheric radiance using the conversion formula from the USGS Landsat program [19, 20]. Furthermore, two images (path 122 row 44, path 122 row 43) of each period were spliced together. To respond to the resolution of the other Landsat instruments (TM, OLI), the MSS images were re-sampled to 30 meters using the nearest neighbor resampling method [21]. The 2009 spliced SR image was used as a reference for registering the other eight spliced images, and the root mean square errors were limited within 0.5 pixels (Table 1).

Since the multi-temporal and multi-sensor images were used, it is necessary to normalize the variation in SR across all used images [22-24]. Comparing the pre-band spectral range, the Landsat time series images have similar or same spectrum range [25], thus iteratively re-weighted multivariate alteration and detection (IR-MAD) transformation [26] was adopted to approximately adjust the differences of SR between used the images of Landsat. We used the 2009 mosaic SR image as a reference for conducting the relative radiometric normalization procedure based on the IR-MAD transformation [25, 26], the atmospheric radiance of the other eight target images (including 1973MSS, 1979MSS, 1988TM, 1994TM, 2000TM, 2005TM, 2013OLI, 2017OLI) were converted to the SR [25-27]. The SR (blue band, green band, red band, near-infrared band, shortwave infrared 1 band, shortwave infrared 2 bands) of 1988TM, 1994TM, 2000TM, 2005TM, 2013OLI, and 2017OLI were corrected with respect to the year 2009 TM SR (blue band, green band, red band, near-infrared band, shortwave infrared 1 band, shortwave infrared 2 bands). For correcting the MSS imagery (three bands analogous to TM) with respect to the year 2009 SR image, the green, red and near-infrared bands of the year 2009 SR image were used to match the SR of the MSS (1973, 1979). Finally, the SR of all used images was approximately adjusted to a common radiometric scale based on the year 2009 SR image.

2.3 Urban landscape classification

We adopted the feature composite classification scheme to extract the urban landscape. First, the normalization different water index (NDWI) and normalization different vegetation index (NDVI) (Equation (1) and Equation (2)) were calculated for the all SR images. Then, NDWI and NDVI images were stacked into the SR image of each study period. Two five-layer images (MSS) and seven eight-layer images (TM, OLI) were obtained to apply classification.

$$NDWI = \frac{B_g - B_n}{B_g + B_n} \quad (1)$$

$$NDVI = \frac{B_n - B_r}{B_n + B_r} \quad (2)$$

where B_g, B_n, B_r represent green, near infrared, and red bands of Landsat imagery.

The urban landscape was broken down into six categories: building, forest, soil, farmland, shrub-grass, and water. All urban landscape classifications were identified using a support vector machines (SVM) technique. Firstly, larger than 1500 points were randomly generated within the overlapped area between the year 2009 TM SR image and the quasi-synchronous high-resolution

image from Google Earth. Then, these points were visually divided as building, forest, soil, farmland, shrub-grass, and water; of more than 200 random sample points for each classification, half of them were employed for validation and the other half were employed for training. The training sample points were employed to train the SVM classifier based on an eight-layers imagery from the year 2009 layer-stacked image [21]. Based on the validation samples, an error matrix was used for evaluating accuracy [28]. The results of accuracy assessment are found in Table 2.

In order to verify whether the five-layers image (green, red, near infrared bands, and NDVI, NDWI images) meet urban landscape classification, a new classifier for the SVM was developed using the same training samples as the eight-layers imagery, whereas only five-layers (green, red, near infrared bands, and NDVI, NDWI images) from the year 2009 layer-stacked image were used. The accuracy was also assessed with the same validation samples, as tabulated in Table 2. Although only five-layers were used, the classified result was similar to the eight-layers SVM approach (Table 2).

Table 2 The accuracy assessment results of the different classification methods (unit: %).

		Water	Building	Soil	Forest	Farmland	Shrub-grass
Eight-layers	Producer's accuracy	96.08	92.00	86.05	90.38	81.13	78.43
	User's accuracy	98.00	92.00	74.00	94.00	86.00	80.00
Five-layers	Producer's accuracy	95.92	90.00	84.78	87.04	80.00	82.35
	User's accuracy	94.00	90.00	78.00	94.00	80.00	84.00

In this study, an elaborated atmospheric correction was employed to minimize the differences between used images (see section 2.2), and to get relatively consistent SR in various Landsat images [23, 26]. Moreover, SVM classifiers (five-layers and eight-layers) generated from the 2009 layer-stacked image is a practical bridge between used images. Therefore, consistent and valid results of classification could be expected using the five-layers SVM classifier for MSS images and the eight-layers SVM classifier for TM and OLI images [21].

2.4 Quantification of landscape responses with urban expansion

A matrix system was generated through a GIS application using classification maps of the region for the years 1973, 1979, 1988, 1994, 2000, 2005, 2009, 2013, and 2017, to quantify how much water, soil, forest, shrub-grass, and farmland were converted directly and indirectly to building. These nine time points enabled the definition of nine conversion episodes, 1973–1979, 1979–1988, 1988–1994, 1994–2000, 2000–2005, 2005–2009, 2009–2013, 2013–2017, and 1973–2017, which could be used to track the process of landscape change due to urban expansion.

2.5 Quantifying the spatio-temporal patterns of urban expansion

The spatial-temporal process of urban expansion was measured from different dimension. We used GIS technique to estimating the types and direction of urban expansion in Guangzhou. Three types of urban expansion were identified using Equation (3) [29, 30]. Urban expansion types are defined as outlying if $S = 0$, edge if $0 < S < 0.5$, and infilling if $S \geq 0.5$. The three expansion types are illustrated in Fig.2.

$$S = \frac{L_c}{p} \quad (3)$$

where L_c is the length of the common edge between a new and existing building patch, and p is the perimeter of the new building patch (Fig.2).

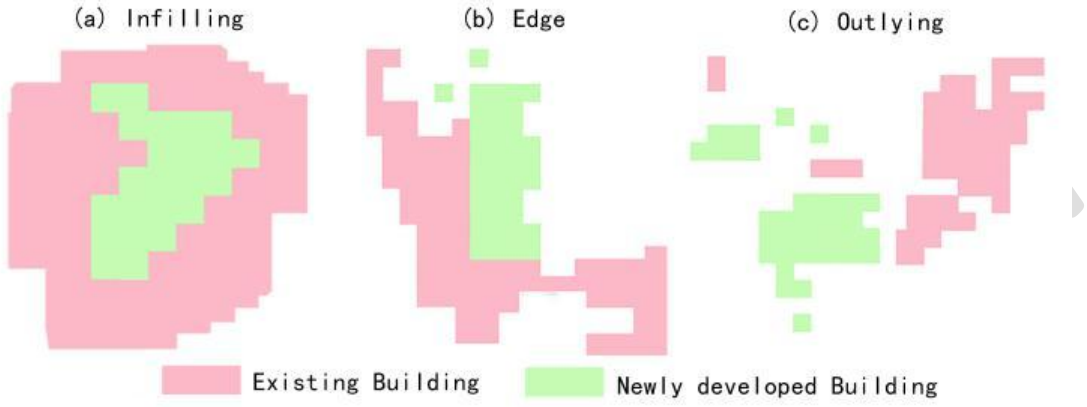

Fig.2 The three types of urban expansion: (a) Infilling, (b) Edge, (c) Outlying.

Urban expansion trajectory was characterized by the changes of Gravity Center (GC). The concept of Gravity Center is used to identify the weighted center of the building, mapping the GC change of the building estimated the spatial direction of urban development [31]. The GC migration was described based on the alteration of the gravity center coordinate (GCC) [31]. The GCC is measured by Equation (4) and Equation (5).

$$X = \frac{\sum_{i=1}^{n} P_i X_i}{\sum_{i=1}^{n} P_i} \quad (4)$$

$$Y = \frac{\sum_{i=1}^{n} P_i Y_i}{\sum_{i=1}^{n} P_i} \quad (5)$$

where X and Y are the GCC for the building, X_i and Y_i are GCC of the ith patch, P_i is area of the ith patch, n is number of patches in the building.

To examine the spatial pattern of expansion and its change over time, four class-level spatial metrics were selected to capture the pattern of three urban expansion types from different dimensions, i.e. the patch density (PD) equals the number of patches of the corresponding patch type divided by total landscape area, the mean patch area (MPA) measure the average area of all patches in the landscape, the landscape shape index (LST) quantify the irregularity of the landscape, and the clumpiness index (CLUMPY) describes the proportional deviation of the proportion of like adjacencies involving the corresponding class from that expected under a spatially random distribution. Four indices describe four key aspects feature of the landscape: density, size, edge, and aggregation respectively. The comments and calculation method of four spatial metrics can be found in the help document of FRAGSTATS software version 4.2.

3 Results

3.1 Landscape responses of urban expansion

The resulting landscape maps generated for the area of study are shown in Fig.3, respectively. During the period 1973–2017, the building areas grew from 0.26% to 23.04% of the study area, the building nearly increased by 90-fold, the change in the area of building indicated that Guangzhou experienced rapid urban expansion over the 44 years period. The building kept on expanding from 1973, the mean annual growth rates of the building also increased greatly, which were 3.83, 5.40, 22.25, 23.34, 47.24, 66.33, 110.60 km^2/year for the seven periods of 1973–1979, 1979–1988, 1988–1994, 1994-2000, 2000-2005, 2005-2009 and 2009-2013, respectively, indicating that the urbanization process of Guangzhou has been accelerated from 1973 to 2013. But the mean annual growth rates of the building decreased during 2013–2017 (101.19 km^2/year), indicating that the speed of urban expansion in Guangzhou tends to slow down.

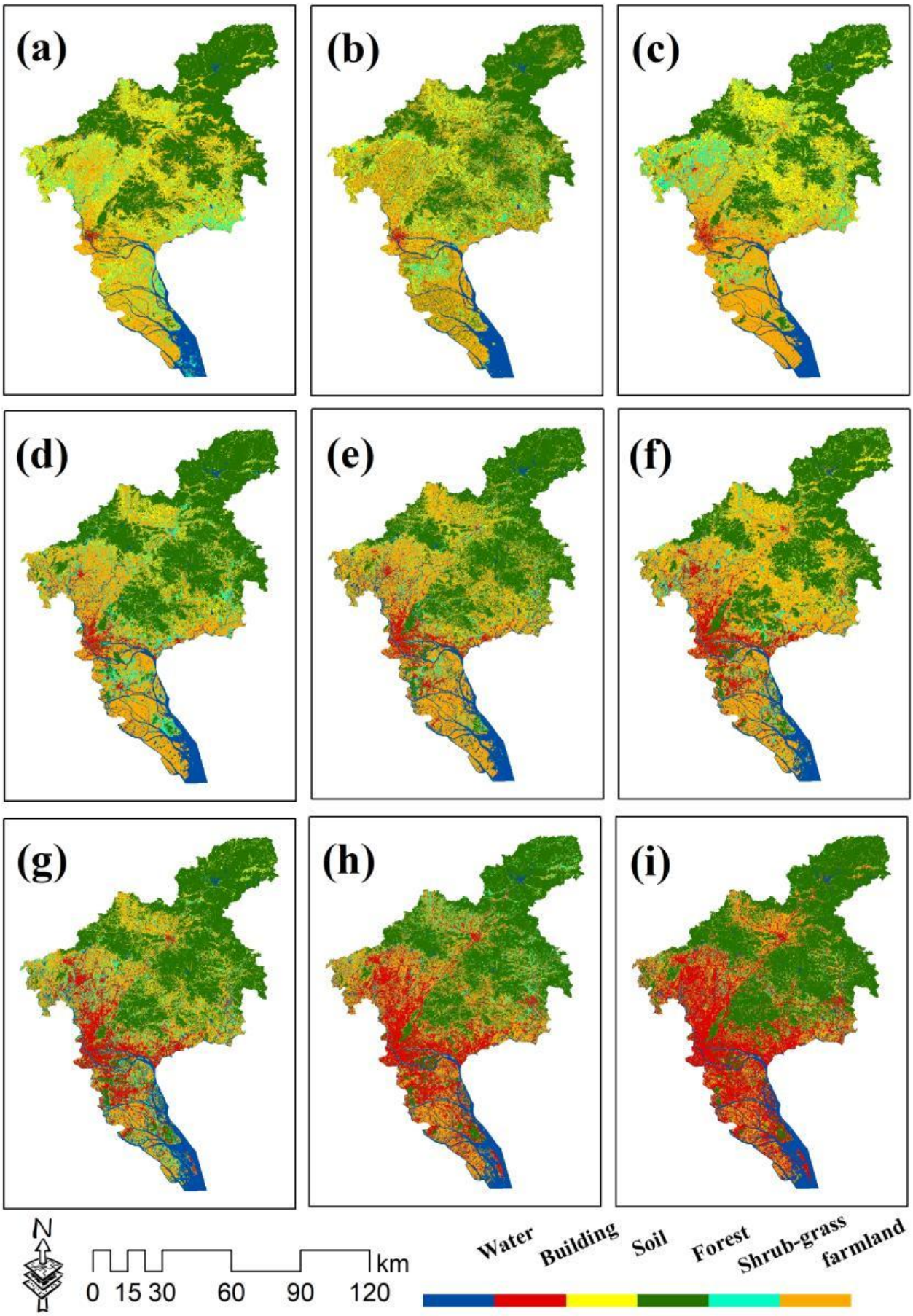

Fig.3 Landscape maps of the studied area for the years: (a) 1973, (b) 1979, (c) 1988, (d) 1994, (e) 2000, (f) 2005, (g) 2009, (h) 2013 and (i) 2017.

The analysis of landscape change revealed a 93.03% decrease in soil, a 66.39% decrease in shrub-grass, a 49.66% increase in water, a 19.76% increase in forest, with a 40.35% decrease in farmland between 1973 and 2017. Urban landscapes have been dramatically changed (Fig.4). The first majority landscape of the study area was forest, the total area of forest fluctuates during these years, but the overall trend is increasing, the forest area in this region in 2017 was 3432.13 km^2, accounting for 46.17% of the total area. The largest area change was found in soil, the soil area drastically reduced during 1973-2017. And the area of soil was falling since 1988. The area of farmland fluctuates during 1973-2005, the area of farmland was falling since 2005, with a high rate of decline over the period of 2005 to 2017. The total area of water fluctuates during whole period, which was found obviously lower in 2000. The total area of shrub-grass fluctuates during these years, but the overall trend is downward.

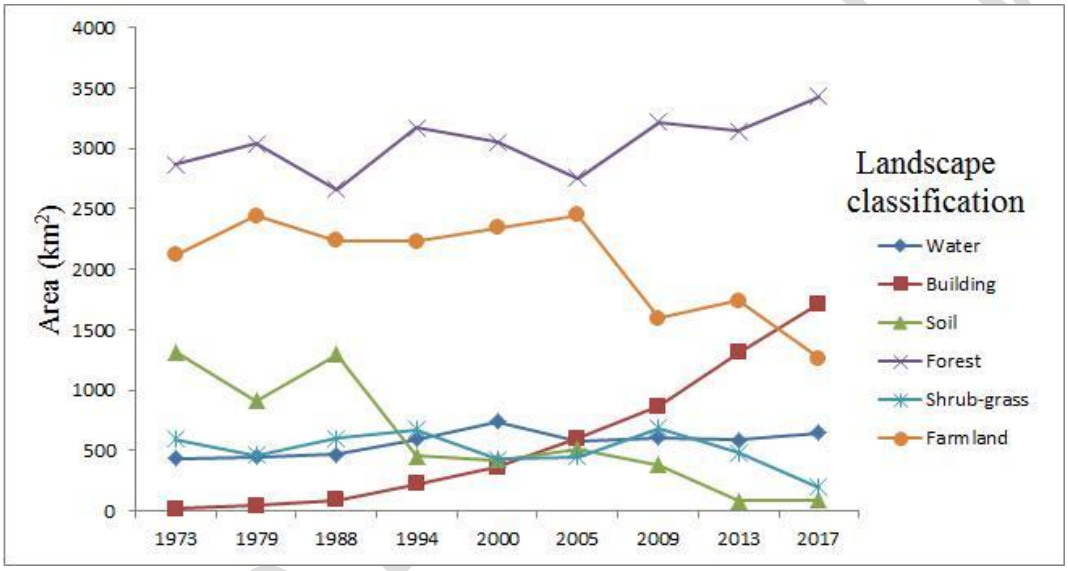

Fig.4 Changes in area of different landscape in Guangzhou from 1973-2017.

The expansion of buildings (+1693.5 km^2) was the leading urban landscape rapidly changing from 1973 to 2017. The other landscape conversion to buildings captured from 1973 to 2017, and the landscape response processes caused by urban expansion are listed in Table 3. Over the period, massive new buildings were developed on land that was previously soil or farmland, with most converted from farmland (807.84 km^2, both directly and indirectly), followed by soil (481.99 km^2, both directly and indirectly). For all study periods, a similar conversion phenomenon was observed, with lots of other landscapes being continuously converted to the buildings.

Table 3 Quantifying landscape responses with urban expansion, based on the other landscapes transferred to buildings from 1973 to 2017 in Guangzhou (unit: km^2).

	Water	Soil	Forest	Shrub-grass	Farmland
1973–1979	0.92	4.40	2.57	1.46	13.60
1979–1988	1.30	11.47	4.80	6.47	24.58
1988–1994	1.59	5.60	10.47	20.21	98.66
1994–2000	4.17	2.68	13.93	52.89	66.38

2000–2005	19.94	7.55	34.53	55.64	118.53
2005–2009	20.43	5.91	36.48	63.75	138.75
2009–2013	22.79	18.70	67.52	161.82	171.56
2013–2017	72.07	2.86	98.76	15.83	215.22
1973–2017	45.32	481.99	134.64	223.67	807.84

3.2 The patterns of urban expansion

Three urban expansion types were identified and the contribution of each in the eight periods was illustrated in Fig.5. Through the 44 years, the edge was the primary expansion type (over 55% in any one period), the landscape surrounding the built up area was gradually eroded because of the edge expansion. In the first period (1973–1979), the infilling type occupied only 3.88% of the total newly developed buildings, while the outlying type occupied 37.11%. In contrast, the percentage of the infilling type increased to almost 31.91% between 2013 and 2017, while the outlying type occupied 10.10%. The areas of infilling expansion were less than the areas of outlying expansion in 1973–1979, 1979–1988, 1988–1994, and 1994–2000, but the areas of outlying expansion were less than the areas of infilling expansion in 2000–2005, 2005–2009, 2009–2013 and 2013-2017. In the period of 2013–2017, the rate of edge and outlying expansion was lower than that in the period of 2009–2013, but the rate of infilling expansion was faster than that in the period of 2009–2013.

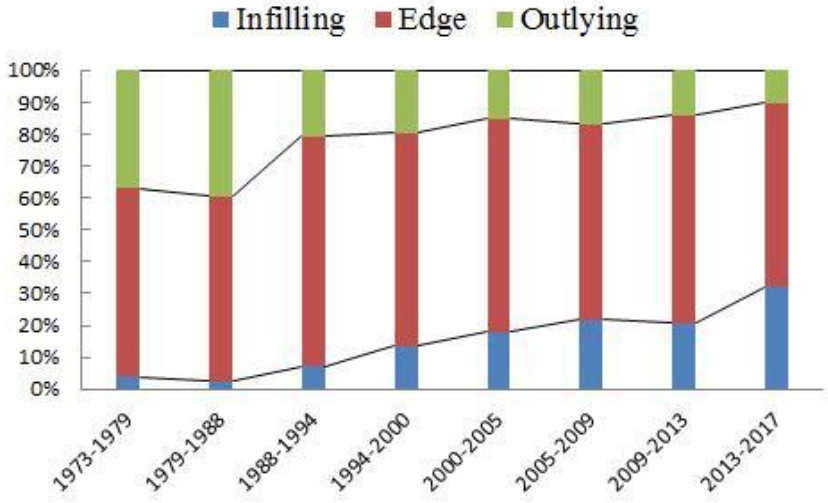

Fig.5 Area percentage of urban expansion type for Guangzhou within the study period.

The GC migration of the building reflected the direction of urban expansion. It can be seen from Fig.6 that the direction of expansion trended toward the northeast of Guangzhou which has large tracts of soil, farmland and forests. With expansion in this direction, a large amount of soil, farmland and forests were replaced by the buildings.

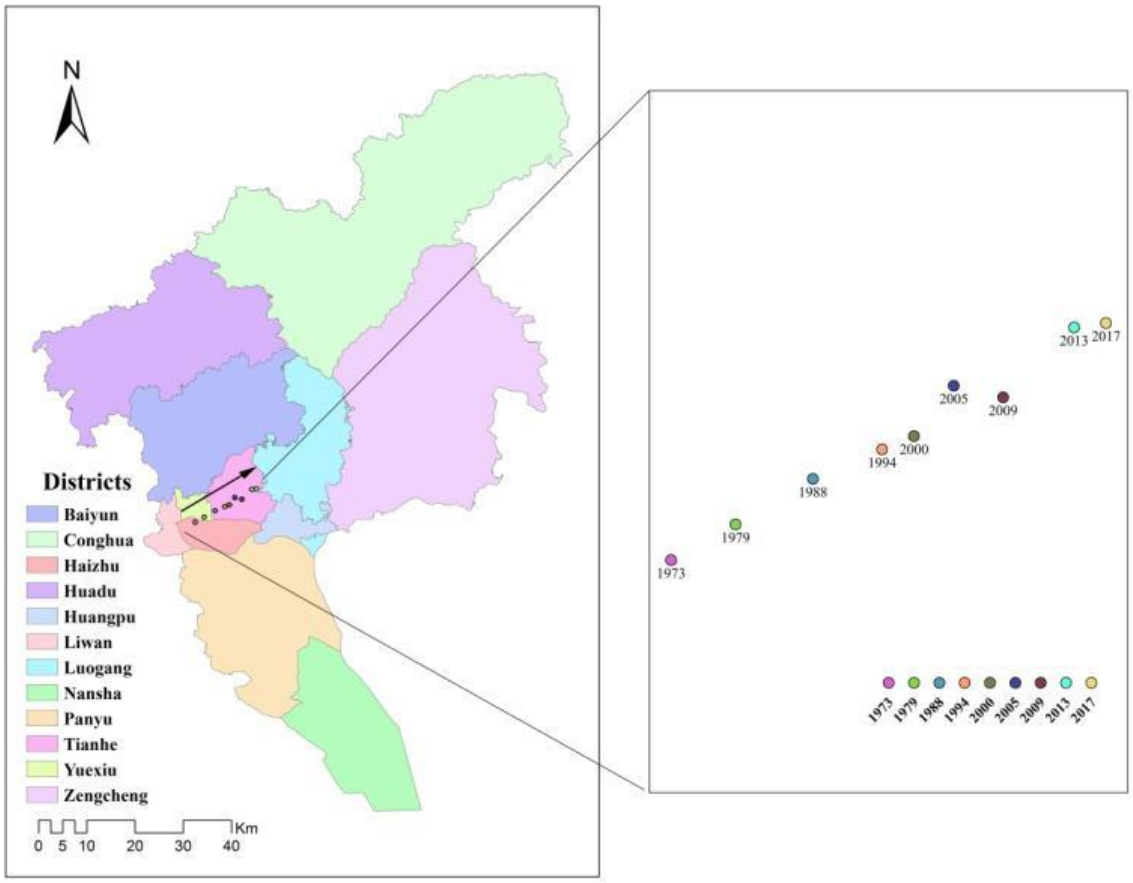

Fig.6 Direction of urban expansion was observed between 1973 and 2017 in Guangzhou.

The metric characteristics shown in Fig. 7 reflect the dynamic patterns of the urban expansion. The MPA of the edge type is higher than the other two types, but the MPA of three expansion types has a slight decreasing trend. The MPA of the infill type decreased from 0.42 ha to 0.32 ha, the edge type also decreased from 1.14 ha to 0.73 ha, and the outlying type also reduced from 0.26 ha to 0.18 ha. The PD of the infill and edge types grew continuously with accelerating urbanization in Guangzhou. The infill type has a higher growth rate than the edge type. The PD of the outlying type reached its peak in 2009-2013 (112.78). The LST of all types increased fleetly, outlying reached its peak in 2009-2013. The CLUMPY of all types declined, the infill and outlying types decreased sharply.

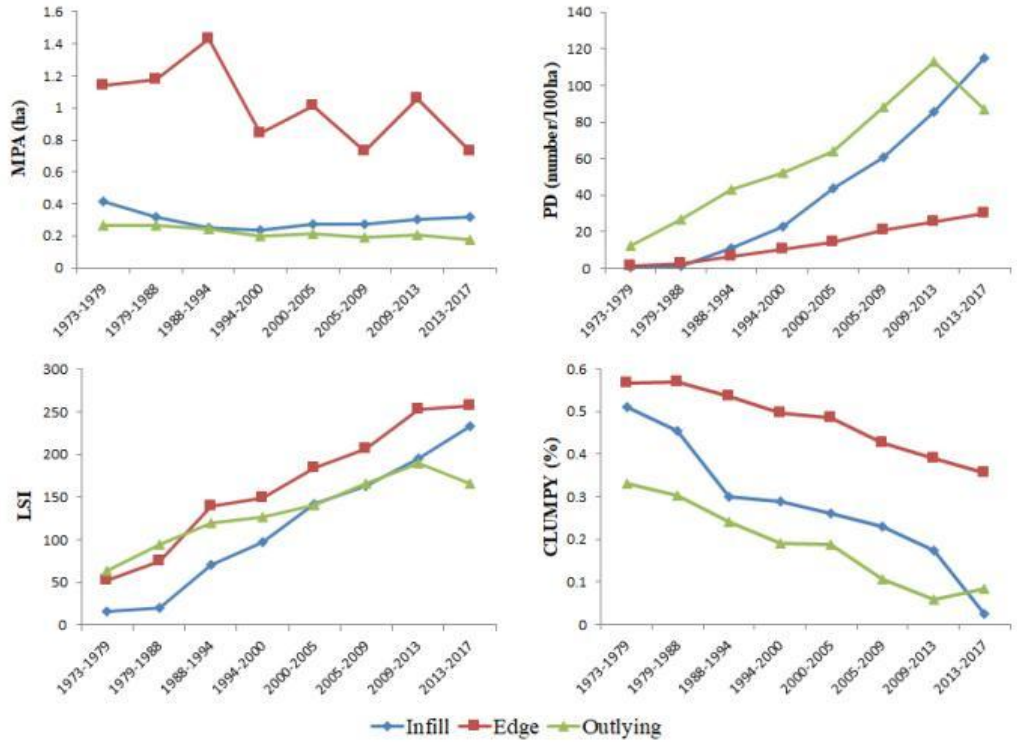

Fig.7 Patterns of three urban expansion types characterized from 1973 to 2017 in Guangzhou.

4 Discussions

This study integrated remote sensing and GIS to analyze the spatio-temporal processes of urban expansion. The IR-MAD transformation was employed to deal with the SR differences between Landsat images, and using the SVM to effectively identify the urban landscape over long-term period. The IR-MAD transformation can reduce the bias caused by different environmental conditions and instruments in the multi-temporal Landsat images [25-27]. Meanwhile, SVM classifiers (five-layered and eight-layered) generated from the same data (2009 layer-stacked image) is a practical bridge between used classification images. The use of consistent training samples can greatly improve the efficiency of mapping urban landscapes. The methodological framework used in this study provides an effectively approach to rapidly extract urban landscape using multi-temporal, multi-sensor Landsat series imagery.

This study evaluated the dynamics of urban expansion and evolution of landscape change and patterns of different expansion types in Guangzhou. Since the reform and opening up in 1978, accompanied by the rapid development of a social economy and the massive increase in population, high-density apartment buildings, industrial parks and urban infrastructure have contributed to rapid urban expansion. The urbanization process, with no signs of slowing down, is the most visible and powerful force that has brought about fundamental transitions in land use and landscape pattern in Guangzhou. As a consequence, the dramatic urban expansion has induced rapid landscape changes. Most of the land surrounding urban areas is used for agriculture. Much of the expansion occurred on the urban fringe along the southwest to northeast direction. Urban expansion through edge erosion therefore occurs mostly at the expense of farmland and the surrounding soil. Spanning the 44 years, the urban landscape pattern underwent rapid changes from being dominated by natural and semi-natural landscape to gradually being dominated by artificial building landscape, resulting in the loss of soil, forests and farmland, and a homogenization of landscape types [6, 32], contributing a significant threat to the services and function of ecosystems in Guangzhou [17, 33]. Durative urban

expansion is projected to impact on landscape pattern in the future [34], there are would grievously threat to the regional ecological security and food security.

Therefore, a key question facing governors now is how to manage urban expansion and its direct and indirect ecological consequences to come up with a sustainable development strategy guiding future directions and optimal patterns of urban land growth to minimize the negative impacts on natural and semi-natural landscape caused by urban expansion in Guangzhou.

The edge expansion was the primary urban expansion type throughout the 44-year period. With the development of time, the proportion of infill type gradually increased, while that of outlying type decreased. This implies that when the growth space has been compressed and the urban form becomes more compact, the main type of urban expansion may gradually turn to infill growth. Comparing the urban expansion patterns of Beijing, Nanjing and Tianjin, we found that the dominating expansion type is significantly different in various urban areas, such as Nanjing with infilling expansion [12], Beijing with both edge expansion and infilling expansion [34], and Tianjin with outlying growth [34]. The regional development conditions and development strategies may contribute to the main causes of these differences. Our results are also significantly different from the result of Sun et al. (2013)[35] in Guangzhou, mainly because the study focused on the core area of Guangzhou.

Urban expansion patterns are a dynamic process in space and time. Four indices were employed to measure the spatial patterns of three types of expansion at different times. Because the edge expansion is dominant, the MPA of the edge expansion is higher than that of the other two types. A decrease in the MPA is an indication that large-scale contiguous building clusters are gradually decreasing, which is also reflected in the decrease of the CLUMP index. The LST of the three expansion types gradually increased, and the majority of patches became more complex and irregular in shape. The combination of increasing patch density and decreasing mean patch area is an indication that the landscape of all expansion types occurring is more fragmented and dispersed. With rapid urban development, the landscape of three expansion types changed dramatically in size and structure, becoming more scattered and more complex configurationally and geometrically.

5. Conclusions

This study focuses on an analysis of the urban expansion pattern and landscape responses of one of China's largest cities, which is rapidly developing. The data produced in this study implied Guangzhou is a highly dynamic region where the landscape has changed dramatically. A large portion of the natural and semi-natural landscape has been converted to buildings since the 1970s, and urbanization has been a major driver of landscape conversion in Guangzhou. Our study provides a more in-depth understanding of the variations in urban expansion patterns in Guangzhou and can be used to optimize the irrational landscape pattern of urban expansion and related issues. It is not only of important theoretical and practical significance to provide necessary geographic information for planning and policy-making, but also for metropolitan area with rapidly growing economies and populations to realize the sustainable use of urban land resources.

Our results point out to the emergence of an expansion process where edge growth sites impact on specific land uses or land covers (soil, farmland, forests, etc.). However, Guangzhou's urbanization process shows no signs of slowing down in the short term. In this state, the edge expansion and outlying expansion should be strictly restricted, and the infilling development should be used as the preferred mode for urban development because it is usually related with a compact urban spatial pattern and edge expansion or outlying expansion model with a scattered one, and the compact

urban spatial pattern has more advantages than the scattered one [34, 36].

Urban landscape change is one of the greatest human impacts on the terrestrial environment. The form of urban development today will control and influence resource use, environmental condition and ecological security in time yet to come. If the urbanized extent is not effectively controlled by land use policy, the constant increase in buildings may be a serious threat to the surrounding natural landscape, and in the near future the urban environment of Guangzhou might reach an irredeemable condition.

For future developments, it is essential that a sustainable land use strategy is produced which will minimize the amount of natural and semi-natural landscapes that will disappear due to urban expansion. Urban authorities should use appropriate land use policies and urban planning to manage the urban land for future sustainable development in Guangzhou.

References:

1. Villa, P., Mapping urban growth using Soil and Vegetation Index and Landsat data: The Milan (Italy) city area case study. *Landscape and Urban Planning* **2012,** *107* (3), 245-254.

2. Weber, C.; Puissant, A., Urbanization pressure and modeling of urban growth: example of the Tunis Metropolitan Area. *Remote Sensing of Environment* **2003,** *86* (3), 341-352.

3. Deng, J. S.; Wang, K.; Hong, Y.; Qi, J. G., Spatio-temporal dynamics and evolution of land use change and landscape pattern in response to rapid urbanization. *Landscape and Urban Planning* **2009,** *92* (3-4), 187-198.

4. Hautier, Y.; Tilman, D.; Isbell, F.; Seabloom, E. W.; Borer, E. T.; Reich, P. B., Anthropogenic environmental changes affect ecosystem stability via biodiversity. *Science* **2015,** *348* (6232), 336-340.

5. Sharifi, A.; Chiba, Y.; Okamoto, K.; Yokoyama, S.; Murayama, A., Can master planning control and regulate urban growth in Vientiane, Laos? *Landscape and Urban Planning* **2014,** *131*, 1-13.

6. Grimm, N. B.; Faeth, S. H.; Golubiewski, N. E.; Redman, C. L.; Wu, J.; Bai, X.; Briggs, J. M., Global Change and the Ecology of Cities. *Science* **2008,** *319* (5864), 756-760.

7. Luck, M.; Wu, J., *Landscape Ecology* **2002,** *17* (4), 327-339.

8. Mitchell, M. G. E.; Suarez-Castro, A. F.; Martinez-Harms, M.; Maron, M.; McAlpine, C.; Gaston, K. J.; Johansen, K.; Rhodes, J. R., Reframing landscape fragmentation's effects on ecosystem services. *Trends in Ecology & Evolution* **2015,** *30* (4), 190-198.

9. Wulder, M. A.; Coops, N. C., Satellites: Make Earth observations open access. *Nature* **2014,** *513* (7516), 30-31.

10. Xie, M.; Wang, Y.; Chang, Q.; Fu, M.; Ye, M., Assessment of landscape patterns affecting land surface temperature in different biophysical gradients in Shenzhen, China. *Urban Ecosystems* **2013,** *16* (4), 871-886.

11. Seto, K. C.; Fragkias, M.; Güneralp, B.; Reilly, M. K., A Meta-Analysis of Global Urban Land Expansion. *PLoS ONE* **2011,** *6* (8).

12. Chen, Y.; Chen, J.; Gao, J.; Yuan, F., Growth Type and Functional Trajectories: An Empirical Study of Urban Expansion in Nanjing, China. *Plos One* **2016,** *11* (2).

13. Gao, J.; Wei, Y.; Chen, W.; Yenneti, K., Urban Land Expansion and Structural Change in the Yangtze River Delta, China. *Sustainability* **2015,** *7* (8), 10281-10307.

14. Alberti, M., Maintaining ecological integrity and sustaining ecosystem function in urban areas. *Current Opinion in Environmental Sustainability* **2010,** *2* (3), 178-184.

15. Li, X.; Yeh, A. G.-O., Analyzing spatial restructuring of land use patterns in a fast growing region using remote

sensing and GIS. *Landscape and Urban Planning* **2004,** *69* (4), 335-354.

16. Chen, Y.; Yu, S., Impacts of urban landscape patterns on urban thermal variations in Guangzhou, China. *International Journal of Applied Earth Observation and Geoinformation* **2017,** *54*, 65-71.

17. Xiong, Y.; Huang, S.; Chen, F.; Ye, H.; Wang, C.; Zhu, C., The Impacts of Rapid Urbanization on the Thermal Environment: A Remote Sensing Study of Guangzhou, South China. *Remote Sensing* **2012,** *4* (7), 2033-2056.

18. Taubenböck, H.; Esch, T.; Felbier, A.; Wiesner, M.; Roth, A.; Dech, S., Monitoring urbanization in mega cities from space. *Remote Sensing of Environment* **2012,** *117*, 162-176.

19. Roy, D. P.; Wulder, M. A.; Loveland, T. R.; C.E, W.; Allen, R. G.; Anderson, M. C.; Helder, D.; Irons, J. R.; Johnson, D. M.; Kennedy, R.; Scambos, T. A.; Schaaf, C. B.; Schott, J. R.; Sheng, Y.; Vermote, E. F.; Belward, A. S.; Bindschadler, R.; Cohen, W. B.; Gao, F.; Hipple, J. D.; Hostert, P.; Huntington, J.; Justice, C. O.; Kilic, A.; Kovalskyy, V.; Lee, Z. P.; Lymburner, L.; Masek, J. G.; McCorkel, J.; Shuai, Y.; Trezza, R.; Vogelmann, J.; Wynne, R. H.; Zhu, Z., Landsat-8: Science and product vision for terrestrial global change research. *Remote Sensing of Environment* **2014,** *145*, 154-172.

20. Yuan, F.; Wu, C.; Bauer, M. E., Comparison of Spectral Analysis Techniques for Impervious Surface Estimation Using Landsat Imagery. *Photogrammetric Engineering & Remote Sensing* **2008,** *74* (8), 1045-1055.

21. Han, X.; Chen, X.; Feng, L., Four decades of winter wetland changes in Poyang Lake based on Landsat observations between 1973 and 2013. *Remote Sensing of Environment* **2015,** *156*, 426-437.

22. Lu, D.; Moran, E.; Hetrick, S., Detection of impervious surface change with multitemporal Landsat images in an urban–rural frontier. *ISPRS Journal of Photogrammetry and Remote Sensing* **2011,** *66* (3), 298-306.

23. Powell, S.; Cohen, W.; Yang, Z.; Pierce, J.; Alberti, M., Quantification of impervious surface in the Snohomish Water Resources Inventory Area of Western Washington from 1972-2006. *Remote Sensing of Environment* **2008**.

24. Song, C.; Woodcock, C. E.; Seto, K. C.; Lenney, M. P.; Macomber, S. A., Classification and Change Detection Using Landsat TM Data. *Remote Sensing of Environment* **2001,** *75* (2), 230-244.

25. Chen, Y.; Yu, S., Assessment of urban growth in Guangzhou using multi-temporal, multi-sensor Landsat data to quantify and map impervious surfaces. *International Journal of Remote Sensing* **2016,** *37* (24), 5936-5952.

26. Canty, M. J.; Nielsen, A. A., Automatic radiometric normalization of multitemporal satellite imagery with the iteratively re-weighted MAD transformation. *Remote Sensing of Environment* **2008,** *112* (3), 1025-1036.

27. Schroeder, T. A.; Cohen, W. B.; Song, C.; Canty, M. J.; Yang, Z., Radiometric correction of multi-temporal Landsat data for characterization of early successional forest patterns in western Oregon. *Remote Sensing of Environment* **2006,** *103* (1), 16-26.

28. Congalton, R. G., A review of assessing the accuracy of classifications of remotely sensed data. *Remote Sensing of Environment* **1991,** *37* (1), 35-46.

29. Wu, Y.; Li, S.; Yu, S., Monitoring urban expansion and its effects on land use and land cover changes in Guangzhou city, China. *Environmental Monitoring and Assessment* **2015,** *188* (1).

30. Xu, C.; Liu, M.; Zhang, C.; An, S.; Yu, W.; Chen, J. M., The spatiotemporal dynamics of rapid urban growth in the Nanjing metropolitan region of China. *Landscape Ecology* **2007,** *22* (6), 925-937.

31. Liu, X.; Dong, G.; Wang, X.; Xue, Z.; Jiang, M.; Lu, X.; Zhang, Y., Characterizing the spatial pattern of marshlands in the Sanjiang Plain, Northeast China. *Ecological Engineering* **2013,** *53*, 335-342.

32. McKinney, M. L., Urbanization as a major cause of biotic homogenization. *Biological Conservation* **2006,** *127* (3), 247-260.

33. Tian, G.; Wu, J., Comparing urbanization patterns in Guangzhou of China and Phoenix of the USA: The influences of roads and rivers. *Ecological Indicators* **2015,** *52*, 23-30.

34. Wu, W.; Zhao, S.; Zhu, C.; Jiang, J., A comparative study of urban expansion in Beijing, Tianjin and Shijiazhuang over the past three decades. *Landscape and Urban Planning* **2015,** *134*, 93-106.

35. Sun, C.; Wu, Z.-f.; Lv, Z.-q.; Yao, N.; Wei, J.-b., Quantifying different types of urban growth and the change dynamic in Guangzhou using multi-temporal remote sensing data. *International Journal of Applied Earth Observation*

and Geoinformation **2013,** *21*, 409-417.

36. Van de Voorde, T.; van der Kwast, J.; Poelmans, L.; Canters, F.; Binard, M.; Cornet, Y.; Engelen, G.; Uljee, I.; Shahumyan, H.; Williams, B.; Convery, S.; Lavalle, C., Projecting alternative urban growth patterns: The development and application of a remote sensing assisted calibration framework for the Greater Dublin Area. *Ecological Indicators* **2016,** *60*, 1056-1069.